Journal of Materials Chemistry

Cite this: J. Mater. Chem., 2012, 22, 5137

www.rsc.org/materials

PAPER

Meso-2,3-dimercaptosuccinic acid: from heavy metal chelation to CdS quantum dots†

Esra Sevinç,[a] F. Sinem Ertas,[b] Gulen Ulusoy,[b] Can Ozen[c] and Havva Yagci Acar*[abd]

Received 9th November 2011, Accepted 9th January 2012
DOI: 10.1039/c2jm15741a

DMSA (*meso*-2,3-dimercaptosuccinic acid) a prescription drug and a heavy-metal chelating agent, is shown to act both as a sulfur source and a capping agent in the aqueous synthesis of CdS quantum dots under mild conditions. Release of sulfur from DMSA depends on the solution pH and the reaction temperature. Combination of 70 °C and pH 7.5 was determined as the best reaction conditions for a well-controlled reaction. Changing the SH/Cd ratio from 2.5 to 7 provides QDs emitting from blue to orange with 6–9% quantum yield with respect to Rhodamine 2B. Viability tests performed with HeLa and MCF-7 cell lines indicate a very low cytotoxicity. Mild reaction conditions and biocompatibility makes these particles valuable candidates for bio applications.

Introduction

Semiconductor quantum dots (QDs) emerged as one of the hottest materials in the last decade or so due to unique size dependent properties and broad application areas extending from laser to energy, sensors to cell labelling and medical imaging.[1–6] The high extinction coefficient, longer lifetime, broad absorption and narrow emission profile of QDs has made them popular alternatives to organic fluorophores and potential imaging agents.[3,7–9]

Biotechnology applications usually require aqueous suspensions of nanoparticles. This is either achieved through transfer of hydrophobic particles into aqueous solutions or direct synthesis of QDs in water.[10–13] Thioglycolic acid (TGA) and 3-mercaptopropionic acid (3-MPA) are the most widely used thiolated ligands in the preparation of aqueous QDs, yet suffer from long term instability due to loss of sulphur.[14,15] Recently, Acar *et al.* reported 2-mercaptopropionic acid (2-MPA) as a better and stable coating.[15] Coating is crucial for chemical and physical properties. During synthesis it moderates the crystal growth allowing size control, passivate surface (which is very important to prevent aggregation, surface oxidation, leaching of heavy metal), and eliminates dangling bonds which cause non-radiative coupling events. Also, the chemistry of the coating molecules determines surface charge and chemistry.

One of the most important drawbacks of quantum dots is the heavy metal toxicity. Cadmium release from CdX (X = S, Se, Te) QDs induces toxicity.[9,16] Therefore, stability of the particles and biocompatibility of the coating are important issues in practical applications of the QDs.

Meso-2,3-dimercaptosuccinic acid (DMSA) is a good heavy metal chelating agent and an FDA approved drug which has been used to treat heavy metal poisoning in the human body since the mid 1950s.[17–20] Since 1975, there have been also numerous studies on ^{99m}Tc-DMSA complexes and their use in medical imaging especially for cancer detection.[21–24]

Most of the studies on DMSA focus on complexation of heavy metals such as arsenic, mercury and lead.[19,25–28] There are several reports on Zn complexes and very few on Cd complexes of DMSA.[17,29,30] These studies are mostly interested in the binding strength, *in vivo* detoxification ability and structure of the complex. Although there is no agreement between the reports, either complexation with two thiolic groups[17] or coordination with one thiol and one carboxylate[29] possibly in a polymeric form[17] were suggested for the Cd/DMSA complexes. DMSA consists of two thiol (pK_{S1} = 9.65 and pK_{S2} = 12.05) and two carboxylic acid groups (pK_{C1} = 2.71 and pK_{C2} = 3.43).[17] Therefore, pH can change the type of complex formed with the heavy metal.[17]

Considering the biocompatibility, tetrafunctional structure, water solubility and ability to complex metal ions, DMSA holds a great potential as a coating for nanoparticles designed for biological applications. There are few studies on DMSA coated iron oxide nanoparticles.[31–35] There is one study on Ag-DMSA[36] but there are no reports for DMSA coated QDs to the best of our knowledge.

[a]*Koc University, Graduate School of Materials Science and Engineering, Rumelifeneri Yolu, Sarıyer, 34450, Istanbul, Turkey. E-mail: fyagci@ku.edu.tr; Fax: +90 2123381559; Tel: +902123381742*
[b]*Koc University, Department of Chemistry, Rumelifeneri Yolu, Sarıyer, 34450, Istanbul, Turkey*
[c]*Biotechnology Dept., Center of Excellence in Biomaterials and Tissue Engineering (BIOMATEN) and Central Laboratory, METU, Ankara, Turkey*
[d]*Koc University, KUYTAM, Rumelifeneri Yolu, Sarıyer, 34450, Istanbul, Turkey*
† Electronic supplementary information (ESI) available. See DOI: 10.1039/c2jm15741a

DMSA is expected to provide good passivization of the CdS surface through thiols and stabilize particles in an aqueous medium through carboxylic acid groups which can also provide electrostatic stabilization. Typical aqueous syntheses of CdS QDs require the use of cadmium salts, Na_2S as a sulfur source and a stabilizing/coating molecule.[13,37,38] Yet, we have discovered that DMSA can act both as a sulfur source and a coating material in the aqueous synthesis of CdS nanoparticles.

Herein, we report the first synthesis of size tunable aqueous CdS QDs using DMSA as the sole sulfur source and a coating material. This will be a practical way of producing aqueous and biocompatible CdS quantum dots. Besides, awareness of the behaviour of DMSA is very important for its future applications.

Materials and methods

Materials

Cadmium acetate dihydrate ($Cd(CH_3COO)_2 \cdot 2H_2O$, 98%), 2-mercaptopropionic acid $C_3H_6O_2S$, ≥96%), thioacetamide (CH_3CSNH_2, ≥99%), Rhodamine B was purchased from Merck. *Meso*-2.3-dimercaptosuccinic acid ($C_4H_6O_4S_2$, ≥97%) was purchased from Fluka. All solutions were prepared in Milli-Q water (Millipore).

Preparation of CdS QDs

Cadmium acetate (53.3 mg, $Cd(CH_3COO)_2 \cdot 2H_2O$) was dissolved in 80 mL water in a three-necked round-bottom flask. Twenty millilitres of DMSA solution prepared by sonication of the required amount of DMSA in water at 70 °C was added to the Cd-solution at room temperature, and then the pH was adjusted to 7.5 with 1 M NaOH under N_2 flow. This Cd/DMSA solution was deoxygenated for 15 min with nitrogen, and then the solution was heated to 70 °C. The amount of DMSA required was expressed as a SH/Cd mol ratio. The SH/Cd ratios between 1.5 and 7 were studied. Each DMSA molecule contains two SH groups. The duration of the reactions depends on the amount of DMSA and shortens as the amount increases. Samples for further characterization were prepared by multiple washing of QDs with water through Amicon 3 K ultra-centrifugal filters at 3800 rpm in order to remove excess organic materials or inorganic ions from solutions. Samples were stored in the refrigerator.

Characterization

Absorbance and emission spectra were recorded with a Schimadzu UV-Vis-NIR spectrophotometer model 3101 PC and Horiba Jobin Yvon-Fluoromax3 spectrofluorometer, respectively. All optical measurements were performed at room temperature under ambient conditions. PL spectra of CdS QDs were recorded in the range of 365–850 nm at a 0.5 nm interval at the excitation wavelength of 355 nm. A 370 nm longpass filter was used for these measurements. PL spectra were all calibrated with respect to absorption values at the excitation wavelength.

Quantum yields were estimated according to the procedure reported in ref. 39 by diluting the samples to three different concentrations having maximum of 0.1 absorbance at the excitation wavelength of 355 nm. Rhodamine B (31% QY in water) was used as reference. Brus Equation[1] was used to calculate the sizes of the CdS-DMSA nanoparticles. Particle concentration was calculated as reported by Peng *et al.*[40] Fourier Transform Infrared (FTIR) spectra were obtained on a Jasco FT-IR-600 spectrometer using KBr pellet of the dried samples. Samples were dried after washing in a Labconco freeze-drier unit. Powder X-ray diffraction (XRD) analysis was performed using a HUBER G670 diffractometer equipped with a germanium monochromatized Cu-Kα radiation ($\lambda = 1.5406$ Å). XPS analysis was performed on a Thermo Scientific K-Alpha XPS with Al K-alpha monochromated radiation (1486.3 eV). A 400 μm spot size was used. The pass energy for scans was 50.0 eV. Flood gun was used for charge compensation. Base pressure better than 3×10^{-9} mbar and experimental pressure of 1×10^{-7} mbar were achieved. All binding energies are with respect to C1s at 285.0 eV. Washed and dried QD samples were places on an Aluminum adhesive tape. Fluorescence lifetime measurements were conducted using FluoTime 200 fluorescence lifetime spectrometer from PicoQuant GmBH (Berlin, Germany). QD sample was excited at 350 nm and emission collected at 470 nm. Measurements were performed in duplicate. Decay data was fitted using a biexponential model in which two lifetime components (τ_1 and τ_2) and their relative weights (A_1 and A_2) are described with the relation: $A_1\exp\left(\frac{t}{\tau_1}\right) + A_2\exp\left(\frac{t}{\tau_2}\right)$.

In vitro cell viability

MCF-7 and HeLa cells were cultured at a density of 5×10^4 cells/well in 96-well plates in DMEM culture medium supplemented with 10% fetal bovine serum and 1% penicillin-streptomycin at 37 °C under 5% CO_2 for 24 h. Then the cells were incubated with QDs at doses between 5–20 μg QD/well (25–100 μg mL^{-1}) for 24 h. Cytotoxicity was evaluated by MTT assay. Cells were cultured with MTT reagent for 4 h, the formazan product was dissolved with DMSO : EtOH (1 : 1) and absorbance was measured on EL ×800 Biotek Elisa reader at 600 nm. The viability of cells incubated with QDs was expressed as percentage of the viability of control cells. Statistical significance of results was analysed by Anova and student's t-test by using SPSS software.

Results and discussion

Synthesis of CdS quantum dots with DMSA

Size tunable synthesis of aqueous CdS nanoparticles was achieved using only cadmium salt and DMSA, indicating that DMSA can perform a dual function under specific synthetic conditions: sulfur source and organic coating (Fig. 1). This behaviour of DMSA is pH and temperature dependent. All Cd-DMSA complexes are sparingly soluble in water and become soluble at around pH 7.0 or at 70 °C. Previously, it was reported that DMSA becomes completely soluble in water at and above pH 5.5.[19] Influence of the reaction temperature on CdS formation is dramatic. The minimum required temperature for nanoparticle formation at pH 7.5 is 50 °C since no CdS was formed below this temperature. CdS formation is accelerated with increasing pH. At pH 8.0, an immediate formation of bulk CdS was observed at temperatures ≥50 °C. Reactions performed at room temperature require pH above 8.5 to produce luminescent

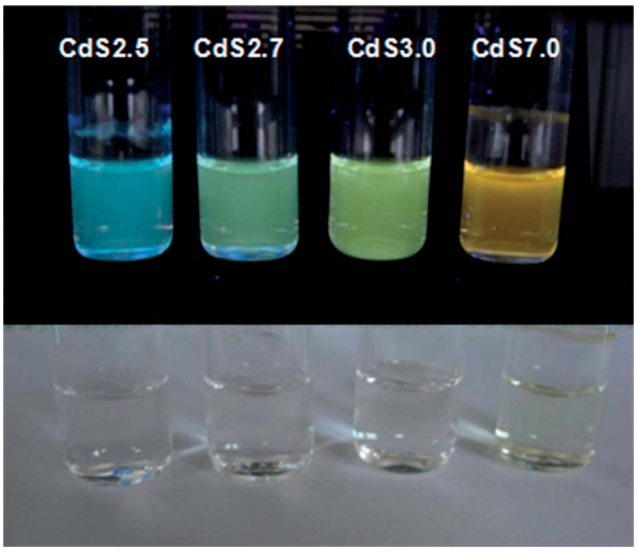

Fig. 1 Photographs of aq. CdS solutions in daylight (bottom) and under UV excitation at 365nm (top).

CdS QDs. At around pH 11, either barely luminescent or bulk particles are formed. However, reactions at room temperature require long reaction times, at least a day or so. At basic pH values, the HS^- concentration decreases (for H_2S, $pK_{a1} \approx 7.0$, and $pK_{a2} \approx 19.0$) and mostly S^{2-} contributes to the CdS formation yielding faster crystal growth.[41] In the case of DMSA, release of sulfur might be increasing with the increasing pH, as well. Considering this interplay between the pH and temperature, pH 7.5 and 70 °C was used to achieve controlled and size tunable synthesis of CdS/DMSA nanoparticles.

Ligand/Cd and Cd/S ratios play a significant role in controlling the size and properties of QDs coated with thiolated molecules.[38] In the case of DMSA, due to its dual function, the SH/Cd ratio is an essential parameter affecting the particle growth and properties. At SH/Cd ratios of 1.5 and 2 (which correspond to Cd excess and stoichiometric balance, respectively) a useful luminescence could not be obtained even though the absorbance onsets are at much lower wavelengths than 516 nm (2.4eV) indicating quantum confinement. At these ratios, DMSA amount may not be sufficient to both supply sulfur and to stabilize the forming crystal effectively. Surface defects may dramatically reduce the luminescence efficiency of such small crystals. Further increase in the DMSA amount produces QDs luminescing from blue to orange with quantum yields around 6–9% (Table 1). Full-width at half maximum (FWHM) does not show a dramatic difference between the particles indicating not a significant difference in size distribution between these particles. A red shift in the absorption and emission peaks is evident with the increasing SH/Cd ratio (Fig. 2A and B). An increased amount of DMSA supplies higher concentration of sulfide ion for growth and more DMSA for coating which controls growth and stabilization. SH/Cd ratio of 2.5 provides a slight excess of DMSA and brings about a major increase in size and a dramatic improvement in luminescence. On the other hand, particle concentration decreased dramatically (Table 1). The highest luminescence intensity obtained at the SH/Cd ratio of 2.7 which caused a small increase in size (green luminescence) and another substantial drop in the particle concentration. Particle concentration stays more or less constant until the ratio increases further to 7 where additional nucleation seems to occur with the large excess of DMSA. This can be interpreted as no additional nucleation but growth between SH/Cd 2.7–3.5 with the increased DMSA amount. Ratio of 3 and 3.5 provided particles of similar quality. Zn and Cd complexes are usually reported as 1/2 or 1/1 ligand/metal complex. Results indicate a need for excess DMSA (Cd being the limiting agent) for effective surface passivization. However, further increase of SH/Cd to 7 resulted in another major increase in the particle size and beyond this ratio, bulk CdS is obtained rapidly. Another important point to note here is that as the DMSA concentration increases, the time required for the CdS formation decreases significantly. For example, while QD formation took about 5 h for the CdS2.5 (SH/Cd = 2.5), it took around 1 h above this ratio.

QY of particles is around 6–9%. Higher QY of smaller particles may be related to better surface quality and less nonradiative couplings due to surface defects (Fig. 3).[42] FWHM and Stokes shift (SS) increases with the particle size (Table 1, Fig. 3). Non-uniform size distribution as well as electron-hole recombination in the intra-band levels due to the defects usually causes such broadening. Increasing SS is usually attributed to strong electron–phonon coupling and increases with decreasing particle size.[43] Yet, for CdS/DMSA an opposite trend is seen. Such reverse trend have been also reported for CdS[44] and ZnO[45] in the literature. Later article relates the phenomenon to Frohlich interaction. However, investigation of such events is beyond the scope of this manuscript.

Table 1 Influence of the SH/Cd ratio on the properties of CdS/DMSA QDs[a]

Sample ID	SH/Cd (mol ratio)	Abs. cutoff (λ) (nm)	PL max. (nm)	Size[b] (nm)	Band gap[c] (eV)	FWHM[d] (nm)	QY[e] (%)	Particle Conc.[f] (mol L^{-1})
CdS1.5	1.5	350	453	2.1	3.55	125	—	—
CdS2.0	2.0	369	447	2.3	3.36	110.5	—	1.37E-05
CdS2.5	2.5	400	472	2.6	3.10	132	8.5	8.73E-06
CdS2.7	2.7	410	504	2.7	3.03	143	8.9	3.57E-06
CdS3.0	3.0	417	522	2.8	2.98	146	7.9	3.50E-06
CdS3.5	3.5	416	519.5	2.8	2.98	148.5	7.9	4.62E-06
CdS7.0	7.0	437	557.5	3.1	2.84	148	6.2	8.18E-06

[a] All reactions were performed at pH 7.5 and at 70 °C. [b] Calculated by the Brus effective mass approximation.[1] [c] Corresponding band gap energy calculated by $E = h\nu$. [d] Full-width at half-maximum calculated from PL spectra. [e] QY calculated according to the procedure of ref. 39 using Rhodamine B as a reference (31% QY in water). [f] Calculated by the method developed by Peng *et al.*[40]

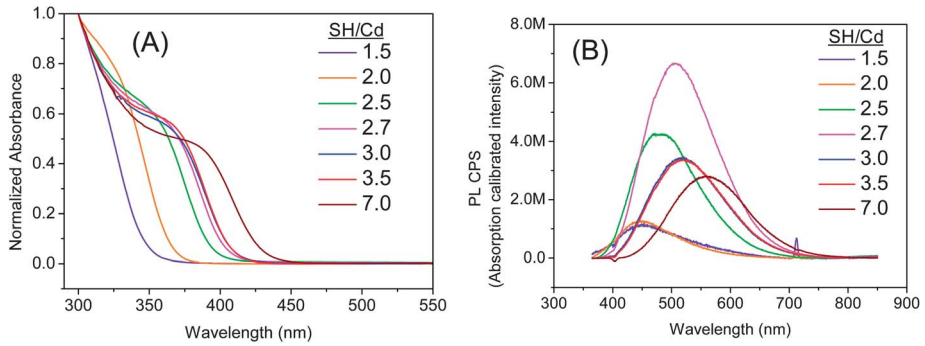

Fig. 2 The evolution of the peak positions of absorbance (A) and, corresponding emission (B) spectra of CdS QDs at different SH/Cd molar ratios. $\lambda_{exc} = 355$ nm. All particles were prepared at pH = 7.5, 70 °C.

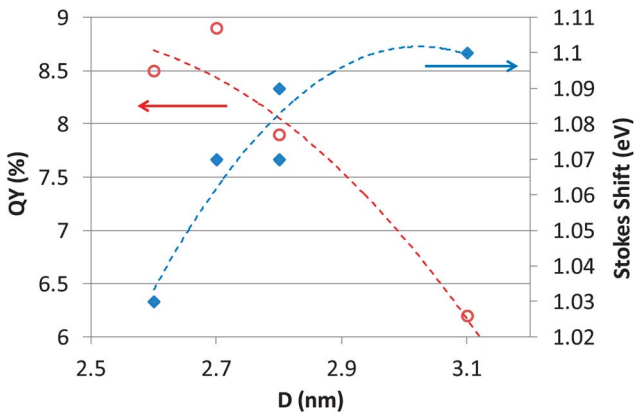

Fig. 3 Relation between the Stokes shift, QY and particle size. Trend lines are just guides for the eye.

These particles exhibit a broad emission profile and large SS similar to many other aqueous CdS reported in the literature.[44,46–48] Usually, such behaviour is related to surface trap emission, which may still show size-dependent luminescence since the energy of trap states may vary with size.[46] Luminescence life-time measurements showed a biexponential decay with a fast ($\tau_1 = 0.6$ ns, $A_1 = 28\%$) and slow component ($\tau_2 = 13$ ns, $A_2 = 72\%$), indicating a greater contribution from trap-state emission (ESI†).[49] SS around 1 eV is usually attributed to cadmium and sulphur vacancies which can act as acceptor or donor defects, respectively.[50–52,53,54] Based on the XPS analysis, Cd vacancy might be the major cause of such large SS which is in agreement with the literature (Tables 2 and 3).[47]

This behaviour of DMSA has never been reported in the literature, most probably because basic pH and heating has never been used together before. In studies where DMSA is used to coat iron oxide nanoparticles, there are no heat treatments and DMSA simply exchanges the initial coating molecule from the surface of iron oxide or bound to the iron oxide surface at room temperature.[35,55] One report indicates polysulfide formation but no details are available.[32] In contrast, DMSA solutions were reported as stable especially under acidic conditions.[19] Aposhian *et al.* investigated the stability of DMSA at pH 5 and 7 at 24 °C by titrating the mercapto units with iodine. Under these conditions after 7 days, pH 5 solutions retained 87% and pH 7 solutions retained 82% of the mercapto groups.[56] However, very recently Stanik *et al.* studied the stability of DMSA under acidic, neutral and basic pH at room temperature and reported formation of fumaric acid as the major degradation product in addition to some oxidized and dimerized DMSA.[57] Instability was reported to be more dramatic under basic conditions but the time scale is from 24 h to 21 days. However, no degradation product was detected for $Sn(DMSA)_2$ complex. In our case, proton NMR studies of the CdS-DMSA did not indicate a significant change in the molecule (data not shown).

Formation of sulfur containing quantum dots through decomposition of the coating is quite scarce in the literature. Cysteine capped CdS has been synthesized through γ-radiation at a ratio of 1/10–1/100 Cd/cysteine[44] in a similar process where CdS is formed from radiolysis of 3-mercapto 1,2-propanediol.[58] However, no quantum yield was reported for comparison of the quality of these particles but size of the CdS QDs are in the range of 3.8–4.5 nm which is larger than the particles obtained here. In a hydrothermal process cysteine was reported to provide sulfur for the Ag_2S formation at long reaction times and temperatures.[59] No structural details are provided.

Structural characterization of CdS-DMSA QDs

In order to obtain information on the structure and composition of QDs XRD, FTIR and XPS analysis were performed. CdS-DMSA QDs have the cubic zinc blende crystal structure. Broadness of the peaks originating from the small crystal sizes

Table 2 Binding energy of the core level electrons for S2p and C3d and corresponding peak areas as measured by XPS

	Peak	Peak BE (eV)	FWHM	% Area
DMSA	$S2p_{3/2}$	162.82	1.36	—
CdS2.5	$Cd3d_{3/2}$	411.72	1.19	—
	$Cd3d_{5/2}$	404.92	1.19	35.89
	$S2p_{3/2}$	163.44	1.11	11.31
	$S2p_{3/2}$	161.99	1.22	37.79
	$S2p_{3/2}$	161.16	1.28	15.02
CdS3.5	$Cd3d_{3/2}$	411.7	1.3	—
	$Cd3d_{5/2}$	404.94	1.3	22.91
	$S2p_{3/2}$	163.59	1.11	28.23
	$S2p_{3/2}$	161.89	1.32	37.37
	$S2p_{3/2}$	161.12	1.34	11.49

Table 3 Ratio of the atoms calculated from XPS analysis

	S_{total}/Cd	S_{CdS}/Cd	S_{CdS}/S_{ligand}
CdS3.5	3.36	2.13	1.73
CdS2.5	1.79	1.47	4.67

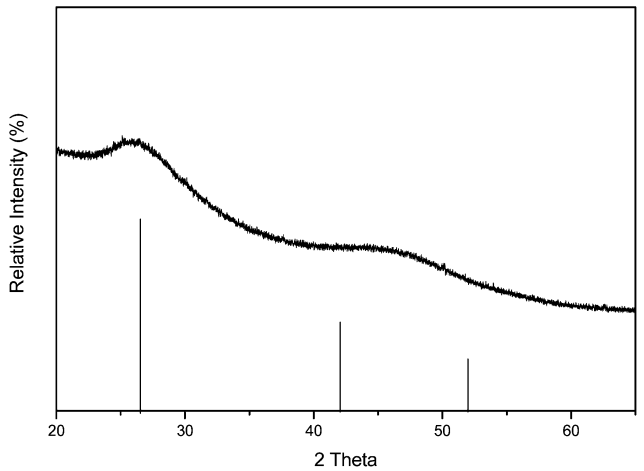

Fig. 4 Powder X-ray diffractogram of CdS2.7.

causes an overlap of the peaks at 42° and 52° in the diffractogram (Fig. 4).

DMSA has the characteristic peaks of S–H at 2564.8 cm^{-1} in the FTIR spectrum (Fig. 5). This peak is still visible in the Cd/DMSA complex at room temperature (SH/Cd = 2.7, pH 7.5) indicating the presence of S–H which completely disappears in CdS-DMSA. This may originate from surface binding of thiols and/or release of sulfur but only after the heating process. DMSA also has the characteristic C=O stretching of the carboxylic acid at 1720.4 cm^{-1} in the FTIR spectrum. Spectra of Cd-DMSA complex and CdS-DMSA show asymmetric and symmetric stretching modes of carboxylate at around 1580 and 1388 cm^{-1}.

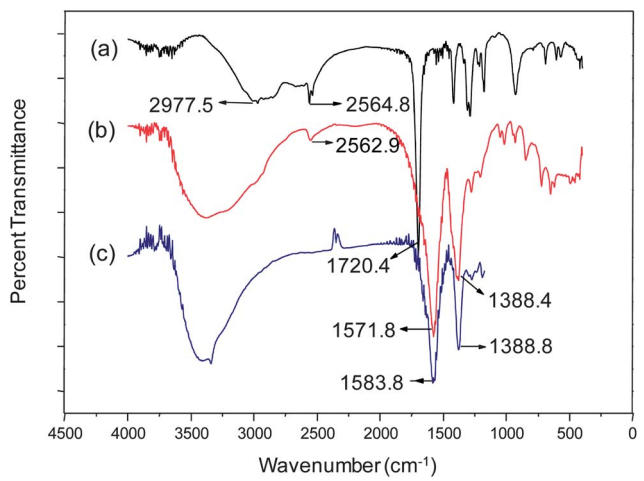

Fig. 5 FT-IR spectra of (a) DMSA, (b) Cd-DMSA complex formed at pH 7.5 and room temperature (RT), (c) DMSA coated CdS QDs (CdS2.7) formed at pH 7,5 and 70 °C.

XPS analysis of the samples show two peaks for Cd 3d due to spin–orbit splitting at 411.7 and 404.9 for $Cd3d_{3/2}$ and $Cd3d_{5/2}$ which corresponds to CdS (Table 2, Fig. 6a).[60,61] The S2p core level was fitted with a doublet (S2p½ and S2p$^3/_2$) due to spin–orbit splitting with a 1.1–1.2 eV separation. CdS nanoparticles coated with DMSA displayed three different binding energies for S2p (Fig. 6b and c). Peaks at 161.1 and 161.8 eV are for sulfides. Two peaks may indicate sulfur at a slightly different environment such as surface *versus* core. Area of the higher BE peak is about 2.5–3.2 times higher than the low BE one, and agrees well with the literature value of CdS, therefore considered as the sulfur of the core CdS.[61] Peak at 163.5eV indicates the presence of S on the ligand. Pure DMSA has a sulfur peak at 162.82 eV and the shift towards higher energy may originate from the surface binding (Fig. 6d). The presence of this type of sulfur also confirms that DMSA still has one sulfhydryl unit even after CdS formation. When peak areas are considered, S/Cd ratio increases as the DMSA/Cd ratio increases (Table 3). Besides S_{CdS}/S_{ligand} decreases as the DMSA/Cd ratio increases indicating the presence of more sulfhydryl group with the excess of DMSA.

Stability of CdS-DMSA QDs

The particles are quite stable if stored in a refrigerator (Fig. 7). However, storage under ambient conditions caused a red shift of the absorbance edge and PL_{max} accompanied with a significant loss of luminescence in 10 days followed by precipitation after 15 days. DMSA could slowly continue to release sulfur at room temperature, increasing the particle size. Yet, further decomposition/oxidation of DMSA, or surface oxidation may finally lead to lack of passivization on the CdS surface, causing uncapped sites, increasing non-radiative events and aggregation. Removal of excess material from the particles did not change the general trend.

Cell toxicity

There is a great concern about using Cd-based QDs for *in vivo* applications due to cadmium toxicity and ROS production.[9] Therefore, the stability of particles, ensuring no or limited release of cadmium is necessary. A good surface passivization, use of a stable coating, or inorganic shell formation may minimize this handicap. Use of DMSA which can be used for cadmium toxicity is indeed expected to pose good cell viability, since it can potentially complex at least some of the Cd^{2+} leaching from the particle.

A routine MTT assay was used to measure the metabolic activity of human cervical (HeLa) and breast (MCF-7) cancer cell lines incubated with 25–100 μg mL^{-1} QD for 24 h. Viability indicated by the cell activity showed a slight decrease with the increasing dose but it was in the range of 99–80% for the whole study (Fig. 8). Toxicity of CdS-DMSA is less than CdS-Cysteine within the given concentration range.[62] HeLa and MCF-7 showed viability around 60 and 75%, respectively, when incubated with 100 μg mL^{-1} CdS-cysteine QDs. At the same dose CdS-DMSA provided around 80% viability for both cell lines. At low doses viability is always better but the difference is still significant. At 25 μg mL^{-1} dose CdS-DMSA caused viability above 95% for both cell lines, but this value drops down to

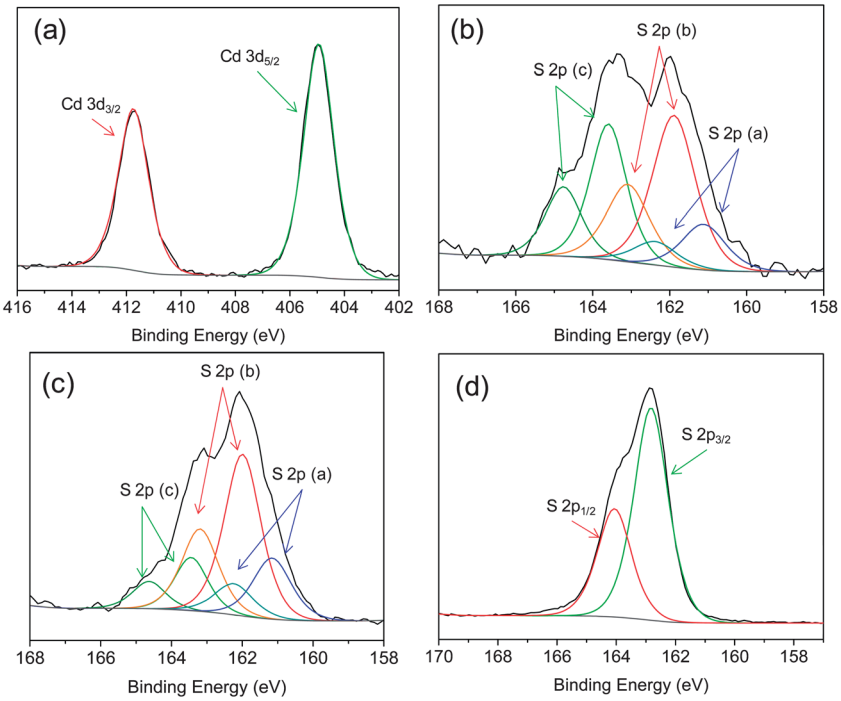

Fig. 6 (a–b) XPS close-up spectra for the Cd 3d and S 2p core level for CdS3.5, (c) S2p core level for CdS2.5, (d) S 2p for DMSA.

80–85% with CdS-Cysteine. Toxicity of the DMSA was also tested at doses 18 and 72 μg mL^{-1} which are much higher than the amount contained in CdS-DMSA QDs based on thermogravimetric analysis (TGA). Particles usually show 40% weight loss up to 600 °C (data not shown) which corresponds to the organic content *i.e.* the coating. MCF-7 cells showed above 90% viability at both doses while HeLa cells showed a dose dependent activity where viability dropped to 74% at the higher dose (Fig. 9). Collectively evaluated with CdS-DMSA results, DMSA doesn't seem to be a major contributor to the observed QD cytotoxicity and DMSA emerges as a very strong alternative to popular cysteine as a biocompatible coating for QDs.

Conclusions

Aqueous CdS QDs were prepared through a novel and very simple procedure using *meso*-2,3-dimercaptosuccinic acid (DMSA) both as a stabilizing agent and a sulfur source in a one pot reaction. Compared to other methods where sulfide release

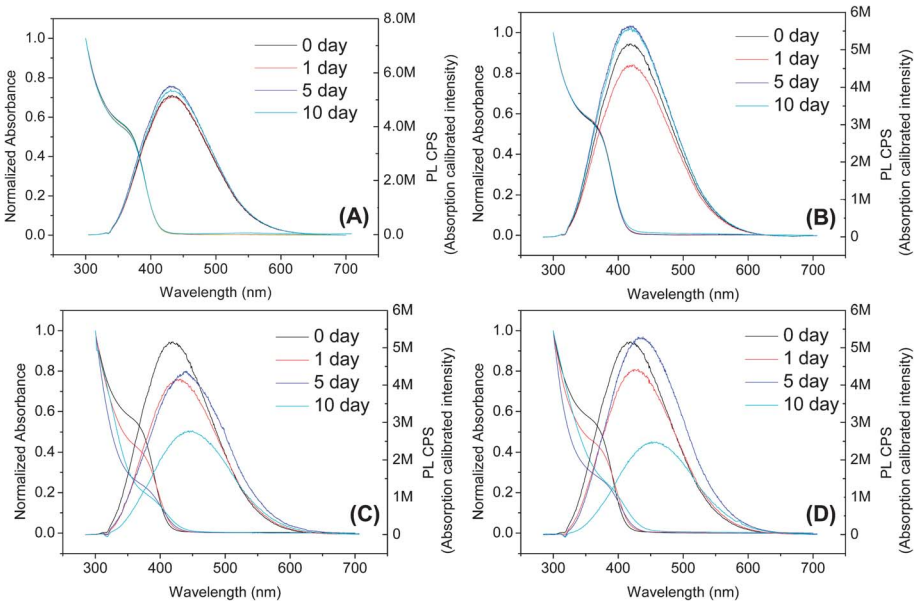

Fig. 7 UV-vis and PL spectra of (A) unwashed, (B) washed QDs stored in a refrigerator and (C) unwashed, (D) washed QDs in ambient conditions.

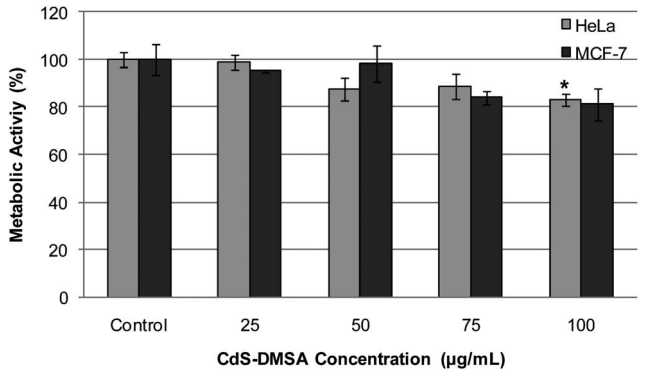

Fig. 8 Cell viability of HeLa and MCF-7 cells as a function of CdS-DMSA QD concentration after 24 incubation measured by MTT assay. (*, significantly different from the respective control value according to student's t-test, $p < 0.05$).

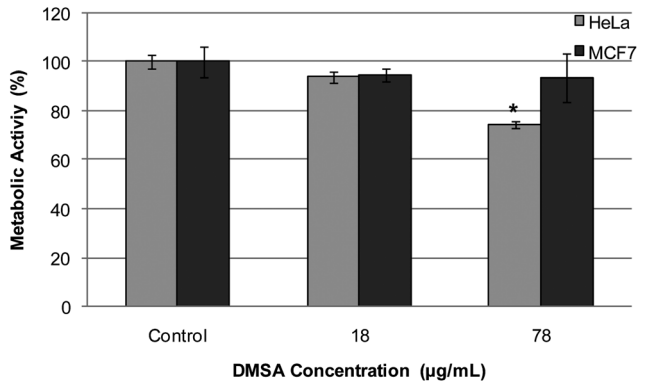

Fig. 9 Cell viability of HeLa and MCF-7 cells in the presence of DMSA after 24 incubation measured by MTT assay. (*, significantly different from the respective control value according to student's t-test, $p < 0.05$).

requires γ-, microwave or photo-irradiation or hydrothermal methods, DMSA offers a very simple and cheap method.[58,63]

Sulfur release from DMSA is shown to be pH and temperature dependent. Although there have been some studies on pH dependent complexes of DMSA, and decomposition, there are no studies in the literature studying the effect of increasing temperature and pH on the stability of DMSA. In a way this is the first of such studies. Low temperature reactions (RT-50 °C) yielded significantly low quality CdS QDs at extended times, and high temperatures lead into quick bulk formation. Therefore, 70 °C and pH 7.5 was determined as the best condition to control particle growth and study other parameters. SH/Cd ratio was effective in controlling the particle size and properties. At and below equimolar amounts of DMSA to cadmium, weakly luminescing, small particles are obtained. Good luminescence obtained only by the excess use of DMSA. Particles which are 2.5 to 3.1 nm with 6–9% QY (relative to Rhodamine B) was synthesized at SH/Cd ratio from 2.5 to 7. However, after the ratio of 7, bulk CdS was obtained rapidly at these reaction conditions. Excess of capping molecules usually is effective in controlling the particle size by surface passivization, yet here it also provides more sulfide therefore increases the particle size.

CdS/DMSA particles showed very high cytocompatibility for HeLa and MCF-7. QY of these particles may not seem very high but it is higher than poly(acrylic acid) coated CdS and many cysteine coated CdS particles which are highly popular as relatively biocompatible QDs.[13,62]

CdS-DMSA QDs show great potential for bio-applications. Perhaps the demonstrated behaviour of DMSA will give a new perspective to the users of DMSA as a nanoparticle coating.

Acknowledgements

The authors thank Koc University for the funding, KUYTAM and Dr Ozgur Birer at Koc University for XPS analysis, Selcuk Acar and Mehmet Somer for XRD, Dr A. Elif Erson Bensan and Dr Sreeparna Banerjee at METU for providing the cell lines, and Urartu Seker and Dr H. Volkan Demir at Bilkent University for the luminescence lifetime measurements.

Notes and references

1 L. E. Brus, *J. Chem. Phys.*, 1984, **80**, 4403–4409.
2 N. Chaniotakis and M. F. Frasco, *Sensors*, 2009, **9**, 7266–7286.
3 R. Dey, S. Mazumder, M. K. Mitra, S. Mukherjee and G. C. Das, *J. Nanomater.*, 2009.
4 C. Burda, A. C. S. Samia and S. Dayal, *Photochem. Photobiol.*, 2006, **82**, 617–625.
5 M. Henini and M. Bugajski, *Microelectron. J.*, 2005, **36**, 950–956.
6 J. M. Costa-Fernandez, R. Pereiro and A. Sanz-Medel, *TrAC, Trends Anal. Chem.*, 2006, **25**, 207–218.
7 M. Green, H. Harwood, C. Barrowman, P. Rahman, A. Eggeman, F. Festry, P. Dobson and T. Ng, *J. Mater. Chem.*, 2007, **17**, 1989–1994.
8 J. F. Weng, X. T. Song, L. A. Li, H. F. Qian, K. Y. Chen, X. M. Xu, C. X. Cao and J. C. Ren, *Talanta*, 2006, **70**, 397–402.
9 S. M. Nie, A. M. Smith, H. W. Duan and A. M. Mohs, *Adv. Drug Delivery Rev.*, 2008, **60**, 1226–1240.
10 M. Y. Gao, S. Kirstein, H. Mohwald, A. L. Rogach, A. Kornowski, A. Eychmuller and H. Weller, *J. Phys. Chem. B*, 1998, **102**, 8360–8363.
11 N. Gaponik, D. V. Talapin, A. L. Rogach, K. Hoppe, E. V. Shevchenko, A. Kornowski, A. Eychmuller and H. Weller, *J. Phys. Chem. B*, 2002, **106**, 7177–7185.
12 H. Zhang, Z. Zhou, B. Yang and M. Y. Gao, *J. Phys. Chem. B*, 2003, **107**, 8–13.
13 S. Celebi, A. K. Erdamar, A. Sennaroglu, A. Kurt and H. Y. Acar, *J. Phys. Chem. B*, 2007, **111**, 12668–12675.
14 G. Y. Lan, Y. W. Lin, Y. F. Huang and H. T. Chang, *J. Mater. Chem.*, 2007, **17**, 2661–2666.
15 H. Y. Acar, R. Kas, E. Yurtsever, C. Ozen and I. Lieberwirth, *J. Phys. Chem. C*, 2009, **113**, 10005–10012.
16 R. Hardman, *Environ. Health Perspect.*, 2006, **114**, 165–172.
17 G. Crisponi, A. Diaz, V. M. Nurchi, T. Pivetta and M. J. T. Estevez, *Polyhedron*, 2002, **21**, 1319–1327.
18 X. F. Zhu and S. Z. Lever, *Anal. Bioanal. Chem.*, 2003, **377**, 666–669.
19 H. V. Aposhian, *Annu. Rev. Pharmacol.*, 1983, **23**, 193–215.
20 H. V. Aposhian, R. M. Maiorino, M. Rivera, D. C. Bruce, R. C. Dart, K. M. Hurlbut, D. J. Levine, W. Zheng, Q. Fernando, D. Carter and M. M. Aposhian, *Clin. Toxicol.*, 1992, **30**, 505–528.
21 F. Al-Saeedi, *Anal. Chem. Insights*, 2007, **2**, 81–83.
22 M. Caglar, N. Yaris and C. Akyuz, *Nucl. Med. Commun.*, 2001, **22**, 1325–1332.
23 J. C. Watkinson, C. R. Lazarus, R. Mistry, O. H. Shaheen, M. N. Maisey and S. E. Clarke, *J. Nucl. Med.*, 1989, **30**, 174–180.
24 N. Ramamoorthy, S. V. Shetye, P. M. Pandey, R. S. Mani, M. C. Patel, R. B. Patel, P. Ramanathan, B. A. Krishna and S. M. Sharma, *Eur. J. Nucl. Med. Mol. Imaging*, 1987, **12**, 623–628.
25 D. E. Glotzer, *Drug Saf.*, 1993, **9**, 85–92.
26 H. V. Aposhian, D. E. Carter, T. D. Hoover, C. A. Hsu, R. M. Maiorino and E. Stine, *Fundam. Appl. Toxicol.*, 1984, **4**, S58–S70.

27 Q. Fang, J. H. Xu, W. T. Yu, S. Y. Guo, D. Xu and M. H. Jiang, *Acta Chim. Sin.*, 1995, **53**, 645–652.
28 X. J. Fang and Q. Fernando, *Chem. Res. Toxicol.*, 1995, **8**, 525–536.
29 M. Rivera, W. Zheng, H. V. Aposhian and Q. Fernando, *Toxicol. Appl. Pharmacol.*, 1989, **100**, 96–106.
30 X. J. Fang and Q. Fernando, *Chem. Res. Toxicol.*, 1994, **7**, 770–778.
31 J. G. Santos, L. B. Silveira, C. Gansau, N. Buske and P. C. Morais, *J. Magn. Magn. Mater.*, 2004, **272–276**, 2330–2331.
32 N. Fauconnier, J. N. Pons, J. Roger and A. Bee, *J. Colloid Interface Sci.*, 1997, **194**, 427–433.
33 M. Auffan, L. Decome, J. Rose, T. Orsiere, M. De Meo, V. Briois, C. Chaneac, L. Olivi, J. L. Berge-Lefranc, A. Botta, M. R. Wiesner and J. Y. Bottero, *Environ. Sci. Technol.*, 2006, **40**, 4367–4373.
34 P. C. Morais, J. G. Santos, L. B. Silveira, C. Gansau, N. Buske, W. C. Nunes and J. P. Sinnecker, *J. Magn. Magn. Mater.*, 2004, **272–276**, 2328–2329.
35 F. Bouyer, L. Maurizi, H. Bisht and N. Millot, *Langmuir*, 2009, **25**, 8857–8859.
36 Y. Negishi and T. Tsukuda, *Chem. Phys. Lett.*, 2004, **383**, 161–165.
37 C. B. Murray, D. J. Norris and M. G. Bawendi, *J. Am. Chem. Soc.*, 1993, **115**, 8706–8715.
38 J. O. Winter, N. Gomez, S. Gatzert, C. E. Schmidt and B. A. Korgel, *Colloids Surf., A*, 2005, **254**, 147–157.
39 J. N. Demas and G. A. Crosby, *J. Phys. Chem.*, 1971, **75**, 991–1024.
40 W. W. Yu, L. H. Qu, W. Z. Guo and X. G. Peng, *Chem. Mater.*, 2003, **15**, 2854–2860.
41 V. Swayambunathan, D. Hayes, K. H. Schmidt, Y. X. Liao and D. Meisel, *J. Am. Chem. Soc.*, 1990, **112**, 3831–3837.
42 A. L. Rogach, T. Franzl, T. A. Klar, J. Feldmann, N. Gaponik, V. Lesnyak, A. Shavel, A. Eychmuller, Y. P. Rakovich and J. F. Donegan, *J. Phys. Chem. C*, 2007, **111**, 14628–14637.
43 A. Joshi, K. Y. Narsingi, M. O. Manasreh, E. A. Davis and B. D. Weaver, *Appl. Phys. Lett.*, 2006, **89**.
44 A. Saha, A. Chatterjee, A. Priyam and S. K. Das, *J. Colloid Interface Sci.*, 2006, **294**, 334–342.
45 R. P. Wang, G. Xu and P. Jin, *Phys. Rev. B.*, 2004, **69**.
46 H. Li, W. Y. Shih and W. H. Shih, *Ind. Eng. Chem. Res.*, 2007, **46**, 2013–2019.
47 M. Molaei, E. Saievar Iranizad, M. Marandi and N. Taghavinia, *AIP Adv.*, 2011, **1**, 012113.
48 W. Lü, Y. Tokuhiro, I. Umezu, A. Sugimura and Y. Nagasaki, *Phys. Status Solidi C*, 2009, **6**, 346–349.
49 S. S. L. Sobhana, M. V. Devi, T. P. Sastry and A. B. Mandal, *J. Nanopart. Res.*, 2011, **13**, 1747–1757.
50 J. Chrysochoos, *J. Phys. Chem.*, 1992, **96**, 2868–2873.
51 O. Vigil, I. Riech, M. GarciaRocha and O. ZelayaAngel, *J. Vac. Sci. Technol., A*, 1997, **15**, 2282–2286.
52 S. Madan, J. Kumar, I. Singh, D. Madhwal, P. K. Bhatnagar and P. C. Mathur, *Phys. Scr.*, 2010, **82**, 045702.
53 N. Chestnoy, T. D. Harris, R. Hull and L. E. Brus, *J. Phys. Chem.*, 1986, **90**, 3393–3399.
54 X. L. Xu, Y. Y. Zhao, E. J. Sie, Y. H. Lu, B. Liu, S. A. Ekahana, X. Ju, Q. K. Jiang, J. B. Wang, H. D. Sun, T. C. Sum, C. H. A. Huan, Y. P. Feng and Q. H. Xiong, *ACS Nano*, 2011, **5**, 3660–3669.
55 P. S. Haddad, T. M. Martins, L. D'Souza-Li, L. M. Li, K. Metze, R. L. Adam, M. Knobel and D. Zanchet, *Mater. Sci. Eng., C*, 2008, **28**, 489–494.
56 H. V. Aposhian, M. M. Mershon, F. B. Brinkley, C. A. Hsu and B. E. Hackley, *Life Sci.*, 1982, **31**, 2149–2156.
57 R. Stanik, J. Svetlik, J. Karlovska and I. Benkovsky, *J. Radioanal. Nucl. Chem.*, 2011, **289**, 909–914.
58 D. Hayes, O. I. Micic, M. T. Nenadovic, V. Swayambunathan and D. Meisel, *J. Phys. Chem.*, 1989, **93**, 4603–4608.
59 J. H. Xiang, H. Q. Cao, Q. Z. Wu, S. C. Zhang, X. R. Zhang and A. A. R. Watt, *J. Phys. Chem. C*, 2008, **112**, 3580–3584.
60 M. Marychurch and G. C. Morris, *Surf. Sci.*, 1985, **154**, L251–L254.
61 G. Hota, S. B. Idage and K. C. Khilar, *Colloids Surf., A*, 2007, **293**, 5–12.
62 S. S. Ozturk, F. Selcuk and H. Y. Acar, *J. Nanosci. Nanotechnol.*, 2010, **10**, 2479–2488.
63 H. T. Chang, G. Y. Lan, Y. W. Lin and Y. F. Huang, *J. Mater. Chem.*, 2007, **17**, 2661–2666.

